Pressure dependence of Raman modes in double wall carbon nanotubes filled with 1D Tellurium

Edgar Belandria [a], *Marius Millot* [b,*], *Jean-Marc Broto* [b], *Emmanuel Flahaut* [c,d], *Fernando Rodriguez* [e], *Rafael Valiente* [f], *Jesus Gonzalez* [e,g]

[a] *Centro de Estudios Avanzados en Optica, Universidad de los Andes, 5201 Mérida, Venezuela*
[b] *Laboratoire National des Champs Magnétiques Intenses (LNCMI) – CNRS UPR 3228, Université de Toulouse, 143 Avenue de Rangueil, 31400 Toulouse, France*
[c] *Université de Toulouse; UPS, INP; Institut Carnot Cirimat; 118, route de Narbonne, F-31062 Toulouse cedex 9, France*
[d] *CNRS; Institut Carnot Cirimat; F-31062 Toulouse, France*
[e] *DCITIMAC-Malta Consolider Team, Universidad de Cantabria, 69005 Santander, Spain*
[f] *Dto de Fisica Aplicada – Malta Consolider Team, Universidad de Cantabria, 69005 Santander, Spain*
[g] *Centro de Estudios de Semiconductores, Universidad de los Andes, Mérida 5201, Venezuela*

A B S T R A C T

The preparation of highly anisotropic one-dimensional (1D) structures confined into carbon nanotubes (CNTs) in general is a key objective in nanoscience. In this work, capillary effect was used to fill double wall carbon nanotubes (DWCNTs) with trigonal Tellurium. The samples are characterized by high resolution transmission electronic microscopy and Raman spectroscopy. In order to investigate their structural stability and unravel the differences induced by intershell interactions, unpolarized Raman spectra of radial and tangential modes of DWCNTs filled with 1D nanocrystalline Te excited with 514 nm were studied at room temperature and high pressure. Up to 11 GPa we found a pressure coefficient of 3.7 $cm^{-1}\,GPa^{-1}$ for the internal tube and 7 $cm^{-1}\,GPa^{-1}$ for the external tube. In addition, the tangential band of the external and internal tubes broaden and decrease in amplitude. All findings lead to the conclusion that the outer tube acts as a protection shield for the inner tube (at least up 11 GPa). No pressure-induced structural phase transition was observed in the studied range.

1. Introduction

The synthesis of mono-dimensional nanocrystals is complex due to the lack of stability of such structures. One way to stabilize them is to prepare them within a container, such as CNTs. CNTs are good candidates for this application due to their inner diameter in the nanometer range, as well as their good chemical and thermal stability [1–3].

Recently, fabrication of nanomaterials with a controllable size and shape has gained great scientific and technological interest, and composite nanostructures, especially core–shell nanostructures, have received intense attention due to their improved physical and chemical properties for electronics, magnetism, optics, and catalysis. Since coaxial nanowires were discovered in 1991 [4], much effort has been made to design rational methods to synthesize one-dimensional core–shell nanostructures, for instance, by laser ablation, chemical vapor deposition and epitaxy, electrophoretic deposition or electrochemical deposition, carbothermal reduction method, layer-by-layer coating and sol–gel methods.

Tellurium (Te), usually in trigonal structure, is a typical p-type narrow gap semiconductor (direct bandgap of 0.35 eV at

* *Corresponding author:* Fax: +33 562 17 2816.
E-mail address: millot.marius@gmail.com (M. Millot).

doi:10.1016/j.carbon.2010.03.036

room temperature) with a unique helical-chain conformation in its crystal structure. Te exhibits a wealth of unique properties such as photoconductivity, nonlinear optical response, thermoelectric, and piezoelectric effect [5] and therefore its thin film and single crystal have wide applications in gas sensors [6], optoelectronic devices [7], and photonic crystal [8,9]. Despite great progresses made in fabrication of various thin films devices, people pay nowadays more and more attention to the devices from 1D nanostructures, primarily because, in the past decade, 1D nanostructures such as nanowires, nanotubes, nanoribbons have become the potential building blocks for construction and integration of functional nanodevices such as field effect transistor (FET) [10], light emitting diodes [11] or ions sensors [12]. FETs are fundamental components of future nanoelectronics due to their high yield and capability to scale down. Some distinctive or superior performances of these 1D nanodevices have been observed compared with those of conventional film and bulk devices [13]. We report in this work the filling of DWCNTs by Tellurium (Te) using a capillary effect technique with melted Te, and their characterization by transmission electron microscopy and micro-Raman spectroscopy under pressure.

2. Experimental

DWCNTs were synthesized by catalytic chemical vapor deposition (CCVD) as described in a previous paper [1]. A systematic analysis of TEM images reveals that samples produced by this method contain approximately 77% of DWCNTs, the high proportion of DWCNTs was also confirmed by electron diffraction with a small admixture of about 18% single wall CNTs (SWCNTs), and roughly 5% triple wall CNTs. The inner and outer diameters range from 0.53 to 2.53 nm and from 1.23 to 3.23 nm, respectively. The median inner diameter is 1.2 nm and the median outer diameter is 1.9 nm [1–3]. They were filled using a high filling yield capillary wetting technique [2]. DWCNTs were mixed and gently ground together with Te powder (99.999% purity, Strem Chemicals). The DWCNT were not deliberately opened prior to filling (no specific treatment was applied in order to achieve this). The co-grinding with Te powder is only intended to obtain a mixture as homogeneous as possible, in mild conditions. No opening should occur during this step. It is thought that at the working temperature (570 °C), the system is dynamic enough to allow distortions at the tube tip and to make the filling possible. Control experiments with DWCNT deliberately opened prior to filling (with other materials) did not show any evidence of improvement of the filling yield.

The mixture was vacuum-sealed in a quartz ampoule which was heated in a programmed furnace at 5 K min^{-1}–843 K (i.e. above the melting point of Te) followed by a dwell at this temperature for 10 h followed by cooling first to 743 K at 1 K min^{-1}, then to 673 K at 0.1 K min^{-1} and then down to room temperature at 1 K min^{-1}. Because of the impossibility to dissolve Te due to its very low solubility in acids, excess of Te located around the DWCNT could not be removed by washing, as this is usually the case with soluble compounds [2,3]. In the case of Te, no suitable condition could be found. The excess of Te is thus partly present in the sample, coating the outside of DWCNT. The final product was still powder-like, there was not enough Te to allow the formation of a CNT-containing Te composite (the density of DWCNT samples is very low and thus the volume of DWCNT powder is much higher than the volume of the Te powder used during the filling experiment). From TEM observations, the DWCNT appear to be exactly as before the filling as far as bundling is concerned: the sample contains both individual DWCNT and small-diameter bundles (typically 20–30 nm maximum). There is no effect of Te in terms of the bundling state of the sample after filling.

Filling yield was roughly estimated to be *ca*. 50%, straight from transmission electronic microscopy (TEM) observations, presented in Fig. 1.

At ambient pressure the Raman spectra of the DWCNTs were recorded in the back-scattering geometry using a micro-Raman, triple grating system (DILOR XY800) equipped with a cryogenic CCD detector. The spectral resolution of the system was about 1 cm^{-1}. For excitation, the 514.5 nm line of an Ar^+-laser was focused on the sample by means of a 100× objective, while the laser power was kept below 2 mW, in order to avoid laser-heating effects on the probed material and the concomitant softening of the observed

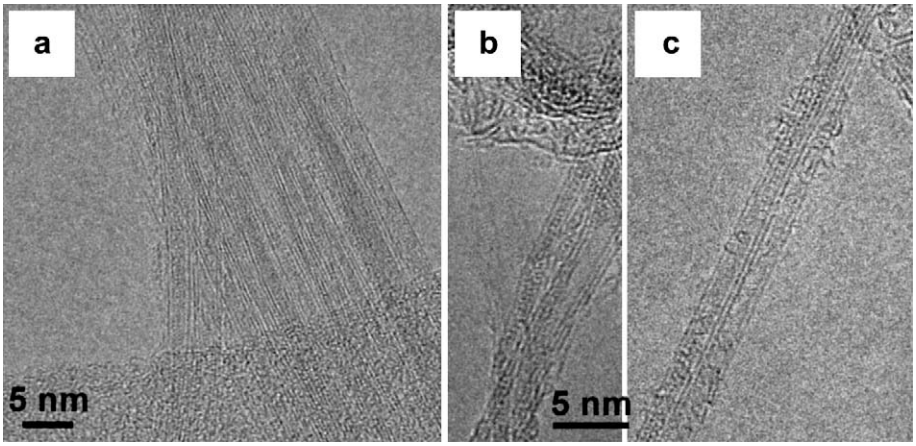

Fig. 1 – TEM images of Te-filled DWCNTs at different magnifications. Te atoms appear as black dots inside the cavity of the DWCNTs.

Raman peaks. High-pressure Raman measurements were carried out using a membrane cylindrical type diamond anvil cell (MDAC). The 4:1 methanol–ethanol mixture was used as pressure transmitting medium and the ruby fluorescence technique was used for pressure monitoring. The DWCNTs were dispersed by ultrasounds in the pressure medium prior to loading. For excitation, the 514.5 nm line of an Ar^+-laser was focused on the sample by means of a 20× objective, while the laser power was kept below 5 mW, measured directly before the cell. The phonon frequencies were obtained by fitting Lorentzian functions to the experimental peaks.

3. Results and discussion

3.1. *Raman scattering at ambient pressure*

In Fig. 2 we present a typical experimental Raman spectrum of Te-filled DWCNTs. We observed the tangential modes (G bands) and the D band which correspond to the double resonance induced by the defects in the CNTs, together with the 2D overtones. The fitted Lorentzian shape peaks for the D and G bands are shown in Fig. 3. The high intensity ratio between the tangential external mode and the D band indicates that the crystalline quality of the nanotubes is rather good. In Table 1 we report the center wavenumbers and full widths at half maximum (FWHM) of the fitted Lorentzian lines. For comparison we have included in Table 2 the values of the fitted Lorentzian lines for pristine DWCNTs, used in the filling process with Te. In the absence of any doping, the G bands of the outer tubes fall in the same spectral range as the G^+ of an isolated semiconducting SWCNT [14–17]. The G band lineshape of pristine DWCNTs is a mixture of Lorentzian lines, the frequencies of the outer tubes (ω_{G+} = 1591 cm^{-1} and ω_{G-} = 1566 cm^{-1}) and a metallic shoulder (ω_{G-} = 1525 cm^{-1}). This is because both the inner metallic (M) and the outer semiconductor (S) tubes are in resonance with the same excitation at 2.41 eV. The Raman spectra of the radial breathing modes (RBM) also confirm that the outer tubes in our DWCNT are semiconducting and the inner tubes are metallic and both are in resonance for the 2.41 eV excitation. From the results of Ref. [18], which establishes the frequency dependence ω_{G-} as a function of diameter (d_t) of the nanotubes, the expected ω_{G-} values for the inner (M) and outer (S) tubes of our DWCNTs are ω_{G-} = 1530 cm^{-1} and ω_{G-} = 1560 cm^{-1} respectively.

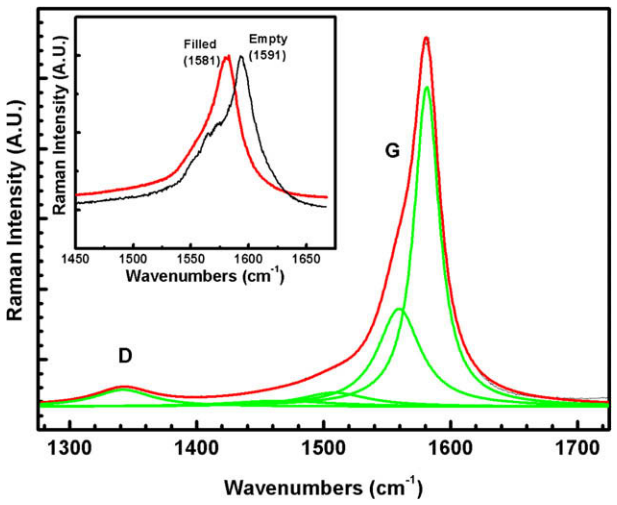

Fig. 3 – Raman spectra at 514.5 nm of the tangential modes and D band, the solid green lines correspond to the fits by Lorentzians. Insert normalized tangential modes of the empty and filled DWCNTs. (For interpretation of the references to colour in this figure legend, the reader is referred to the web version of this article.)

We used the average values of the inner and outer diameters (d_t) of the nanotubes (1.2 and 1.9 nm respectively) obtained by TEM [1–3]. As compared with our experimental values reported in Table 2, there is a good agreement for the outer (S) tube frequency (1566 cm^{-1}) and for the inner (M) tube frequency (1525 cm^{-1}).

The frequencies of the tangential modes of the filled DWCNTs are red shifted with respect to the empty one values. From the values reported in Tables 1 and 2 we can calculate

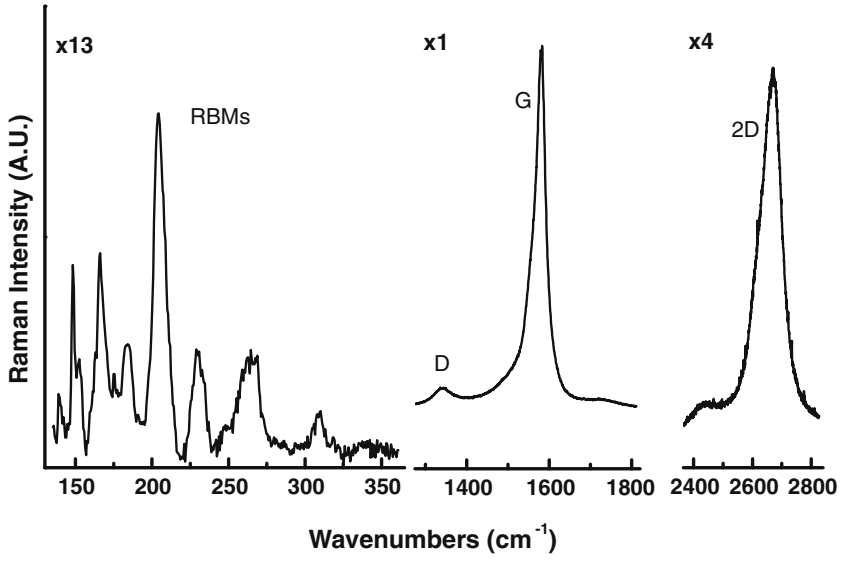

Fig. 2 – Raman spectrum at 514.5 nm and 300 K for Te-filled DWCNTs.

Table 1 – D and G band phonon wavenumber and FWHM in Te-filled DWCNTs from Lorentzian lineshape fits.

Wavenumber (cm^{-1})	FWHM (cm^{-1})
1342 (D)	55.4
1508 (inner metallic G^-)	65
1559 (outer G^-)	40
1581 (outer semiconductor G^+)	24

Table 2 – D and G band phonon wavenumber and FWHM in pristine DWCNTs from Lorentzian lineshape fits.

Wavenumber (cm^{-1})	FWHM (cm^{-1})
1346 (D)	50.4
1525 (inner metallic G^-)	56
1566 (outer G^-)	39
1591 (outer semiconductor G^+)	26

the downshifts of the G bands: 10 cm^{-1} for the G+ outer (S) tube, 7 cm^{-1} for the G- outer (S) tube and 17 cm^{-1} for the G- inner (M) tube. This effect is attributed to the charge transfer between the electrons (n doping) of Te nanowires and the inner walls of the CNTs (see insert in Fig. 3) which produces the softening of the C–C bonds. The blueshift of the G band upon doping reported in references [14,15] results from the contraction and stiffening of C–C bonds. A similar red shift of the tangential modes which is produced by the charge transfer between the electrons of Fe nanowires and the walls of the CNTs is observed if we fill the DWCNTs with α-Fe [16].

Fig. 4 shows the spectral region of radial breathing modes (RBM) measured with 514.5 nm (2.41 eV) excitation, corresponding to outer and inner shells of the DWCNTs. As observed the diameters are ranging from 0.7 nm (inner) to 1.7 nm (outer). Table 3 shows the frequencies and the FWHM

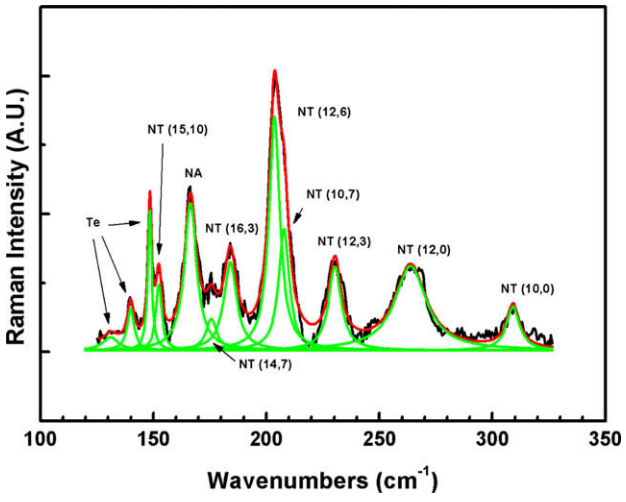

Fig. 4 – Raman spectrum of the radial breathing modes (RBM) of the inner and the outer shells of filled DWCNTs using the 514.5 nm laser line. Solid green lines correspond to Lorentzians fits. (For interpretation of the references to colour in this figure legend, the reader is referred to the web version of this article.)

of the Lorentzian fitted lines attributed to the RBM modes, as well as the calculated chiralities and diameters [17]. The inner and the outer tubes of a DWCNT can be either metallic (M) or semiconducting (S), therefore there are four possible combinations, that we can label as usually: M–M, M–S, S–S and S–M, where S–M indicates an S inner and M outer tube. Hence in Table 3 we can see that there are two simultaneously in resonance at 2.41 eV: inner metallic (M) and outer semiconducting (S) with diameters of 0.94 and 1.7 nm respectively (M–S) and inner semiconducting (S) and outer semiconducting (S) with diameters 0785 and 1.445 nm respectively (S–S). We can also observe the existence of some SWCNTs in agreement with the results of transmission electron microscopy in pristine DWCNT. The frequency 176 cm^{-1} was not assigned (NA) because it did not correspond to nanotubes of chiral indices which have van Hove singularities in agreement with the Kataura plot at 2.41 eV. It may originate from the change in the band structure of the filled nanotubes, but it is not possible to affirm it only through Raman spectroscopy. In this zone, three phonon modes are observed corresponding to Tellurium, at 131, 140 and 148 cm^{-1}. The bulk Tellurium crystallizes in the space group D^4_3 (or D^6_3) with three atoms per unit cell arranged helically about the *c*-axis. The phonons at the center of the Brillouin zone correspond to one Raman-active A_1 singlet (120.4 cm^{-1}), one infrared-active (extraordinary ray) A_2 singlet, and two Raman and infrared-active (ordinary ray) E doublets at 92.2 and 140.7 cm^{-1} respectively [19]. The high energy *E* mode is degenerated, however, here the confinement breaks this degeneracy and allows three modes in the Tellurium nanowires to be detected. To analyze the changes in the region of the radial modes when we fill the CNTs with nanowires of Te, we have included in Fig. 5 the Raman spectra of the radial breathing modes (RBM) measured with 2.41 eV excitation, corresponding to outer and inner shells of the pristine DWCNTs. In the Table 4 we show the corresponding wavenumbers and the FWHM of the Lorentzian fitted lines attributed to the RBM modes, as well as the calculated chiralities and diameters for the pristine DWCNTs. The evolution of Raman spectra upon charge transfer is well accounted for by changes of Raman resonance conditions. In fact when there is charge transfer in CNTs (n or p-doping) there is a change in the electronic band structure (van Hove singularities) which produces a shift in the energy of the Fermi level (E_F) and a loss of resonance conditions. The Raman intensity of a specific CNT (n,m) depends on the resonance conditions. Ref. [14] clearly shows that the loss of resonance takes place gradually and continuously as a function of the E_F shift. Comparing the Raman spectrum of Fig. 4 (Te n-doping DWCNTs) with the spectrum in Fig. 5 (pristine DWCNTs), we generally observe a decrease of the intensities of the radial modes excited at 2.41 eV in DWCNTs filled with Te, because of the loss of resonance produced by charge transfer (n-doping) of the Te nanowires into CNTs. On the other hand the RBM modes frequencies of the inner and outer DWCNTs filled with Te (Fig. 4) are not influenced.

3.2. *Raman scattering under pressure*

In the diamond anvil cell, due to the geometric constraints and the microscope objective of long working distance the

Table 3 – RBM on Te-DWCNTs excited at 514.5 nm.

ω (cm^{-1})	FWHM (cm^{-1})	Chiral Indices	Diameter (nm)	Type	Inner/outer
131	8.3	Te			
140	3.8	Te			
148	2.1	Te			
152	3.2	NT(15.10)	1.70	Semiconductor	Outer
166	6.6	NA			
176	5.8	NT(14.7)	1.45	Semiconductor	Outer
184	6.9	NT(16.3)	1.38	Semiconductor	Single wall
204	5.8	NT(12.6)	1.24	Metallic	Single wall
208	5.7	NT(10.7)	1.16	Metallic	Single wall
230	6.8	NT(12.3)	1.08	Metallic	Single wall
264	16.9	NT(12.0)	0.94	Metallic	Inner
309	7.0	NT(10.0)	0.79	Semiconductor	Inner

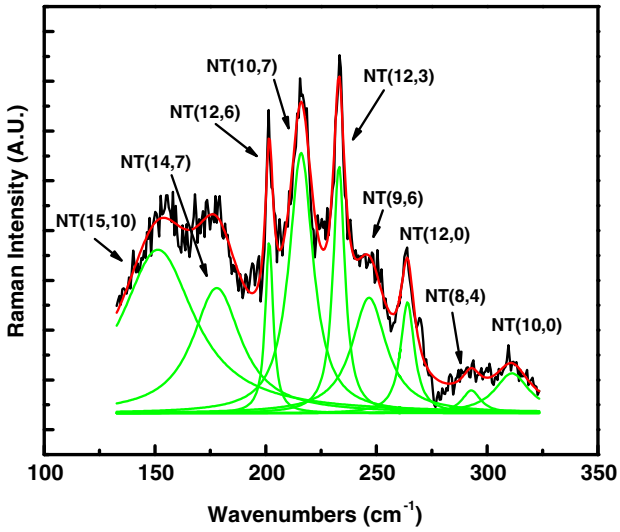

Fig. 5 – Raman spectrum of the radial breathing modes (RBM) of the inner and the outer shells of pristine DWCNTs using the 514.5 nm laser line. Solid green lines correspond to Lorentzians fits. (For interpretation of the references to colour in this figure legend, the reader is referred to the web version of this article.)

intensity of the low frequency radial breathing modes (RBMs) and the Tellurium Raman-active phonons were too low to be observed (spectral range 70–300 cm^{-1}). Fig. 6 shows the Raman spectra as a function of applied pressure in the high frequency range obtained using the methanol-ethanol pressure medium. The G band in DWCNTs contains contributions from both the internal and external tubes, which depend on external parameters such as pressure, temperature, and applied electrical field [20]. We observe a splitting of the G band, the in-plane optical zone centre phonon mode of graphite. The splitting can be attributed to the internal and external tubes [20]. As observed with increasing pressure, the tangential modes shift towards higher wavenumbers. In addition, the tangential bands of the external and internal tubes broaden and decrease in amplitude.

The Raman peaks show a linear dependence up to 11 GPa and the fitting equations are presented in Eqs. (1) and (2) for the filled tubes and Eqs. (3) and (4) for the empty ones, where the wavenumber is expressed in cm^{-1} and the pressure in GPa:

$$\omega_{G(outer)} = 1594 + 7.08p \quad (1)$$

$$\omega_{G(inner)} = 1585 + 3.73p \quad (2)$$

$$\omega_{G(outer)} = 1596 + 5.70p \quad (3)$$

$$\omega_{G(inner)} = 1584 + 3.15p \quad (4)$$

In the diamond anvil cell, as the profile of the Raman modes strongly depends on pressure, it is extremely difficult to properly determine the exact number of peaks necessary to fit each Raman response. This appears to be a consequence both of the extreme broadening of the peaks and evolution of their relative intensities under pressure. Hence we fitted (nonlinear least square) the spectra with two Lorentzians and a constant background as in Ref. [21]. Therefore the zero pressure values obtained in air (Tables 1 and 2) are not comparable to the values obtained from the fits of the spectra

Table 4 – RBM on pristine DWCNTs excited at 514.5 nm.

ω (cm^{-1})	FWHM (cm^{-1})	Chiral indices	Diameter (nm)	Type	Inner/outer
151	40	NT(15.10)	1.70	Semiconductor	Outer
177	27	NT(14.7)	1.45	Semiconductor	Outer
184	6.9	NT(16.3)	1.38	Semiconductor	Single wall
202	4	NT(12.6)	1.24	Metallic	Single wall
208	13	NT(10.7)	1.16	Metallic	Single wall
233	6.4	NT(12.3)	1.08	Metallic	Single wall
264	7.4	NT(12.0)	0.94	Metallic	Inner
293	10	NT(8.4)	0.83	Semiconductor	Inner
311	18.7	NT(10.0)	0.79	Semiconductor	Inner

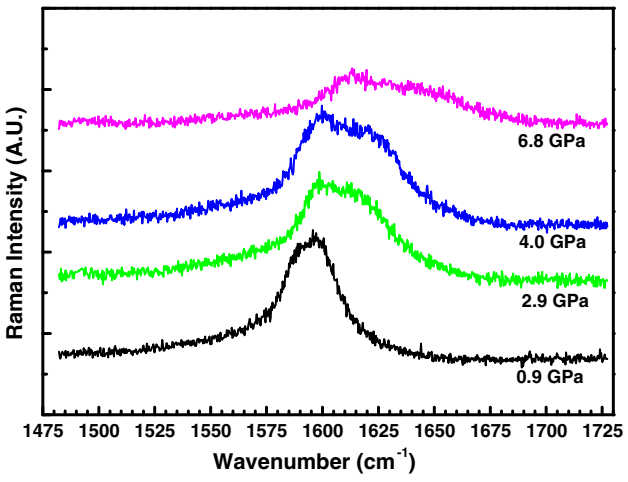

Fig. 6 – Raman spectra at different pressures in the upstroke of Te-filled DWCNTs.

under pressure (Eqs. (1)–(4)). However we have a very good accuracy in the determination of the pressure coefficients of the tangential bands.

The fitted band positions are shown as a function of external pressure in Fig. 7. For comparison we have included the data corresponding to pristine empty DWCNTs. As noted the pressure coefficients of external shells are larger than the coefficients of the inner ones. The external walls do not transmit all the applied load to the internal tubes and as a result the pressure coefficient is expected to be reduced. In addition, under pressure the tangential band of the external and internal nanotubes broadens and decreases in amplitude. It is clear that the tangential band of the external shells broadens much faster than the internal shells, reflecting again the larger deformation of the outer CNTs and the pressure screening for the internal ones. Similar behavior results were previously reported for DWCNTS with a very similar distribution of diameters and the same pressure transmitting medium [21,22].

The values of the frequencies at atmospheric pressure and the linear pressure coefficients for external and internal tangential modes of pristine DWCNTs reported in Eqs. (3) and (4)

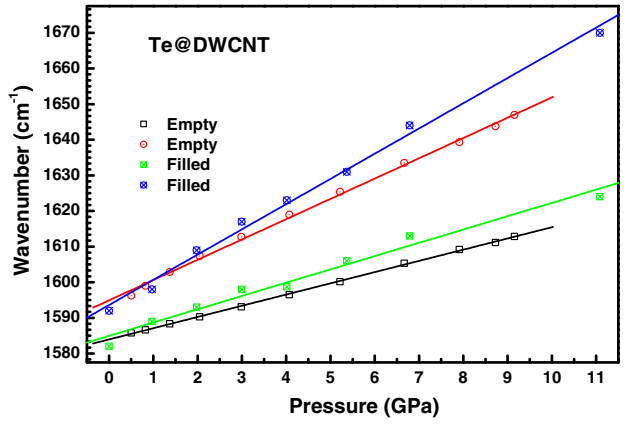

Fig. 7 – Pressure dependence of inner and outer shells of Te-filled DWCNTs.

are close to the values published in Ref. [21] (1595 cm^{-1}, $\partial\omega/\partial P = 5.9\ cm^{-1}\ GPa^{-1}$, 1585 cm^{-1} and $\partial\omega/\partial P = 3.11\ cm^{-1}\ GPa^{-1}$) and [22] (1592 cm^{-1}, $\partial\omega/\partial P = 6.1\ cm^{-1}\ GPa^{-1}$, 1579 cm^{-1} and $\partial\omega/\partial P = 3.3\ cm^{-1}\ GPa^{-1}$. The G band position of the inner tube under pressure is found to be close to the G band observed for graphite [23] but the pressure coefficient is significantly lower than the one reported in graphite (4.7–4.8 $cm^{-1}\ GPa^{-1}$). As observed in Eq. (3) the pressure coefficient of the outer empty CNT is comparable to what has been found for SWCNTs which is about 5.8 $cm^{-1}\ GPa^{-1}$ [24]. It is important to stress that the pressure coefficient of the tangential modes of Te filled CNTs is greater than the pressure coefficient of the empty nanotubes. As we noted above (Fig. 3) there is a charge transfer (n-doping) between the Te nanowires and the CNTs and this doping increases the pressure coefficient of the internal and external modes [25,26]. Under pressure the softening of the C–C bonds due to the transfer of electrons from the Te nanowires to the CNTs causes an increased in the pressure coefficients of the internal and external tangential modes when compared with the ratios of empty nanotubes. The same behavior has already been observed in high-pressure Raman spectroscopy studies in DWCNTs filled with alpha-Iron (α-Fe) nanowires, unraveling a charge transfer (n-doping) from the Iron to the nanotubes [25]. On the other hand, upon p-doping the G band is blueshifted owing to the contraction and stiffening of C–C bonds [25]. Therefore in this case pressure coefficients of the tangential modes for both inner and outer tubes are lower [26].

All findings lead to the conclusion that the outer tube acts as a protection shield for the inner tube (at least up to 11 GPa). No structural phase transitions was not observed in this range of pressure.

Between 11 and 25 GPa we increased the pressure rapidly and then measured the Raman spectrum of the recovered sample. We observed irreversible changes: the frequency of the tangential modes (inner and outer) increases significantly (22 and 13 cm^{-1} respectively) and the D band increases its

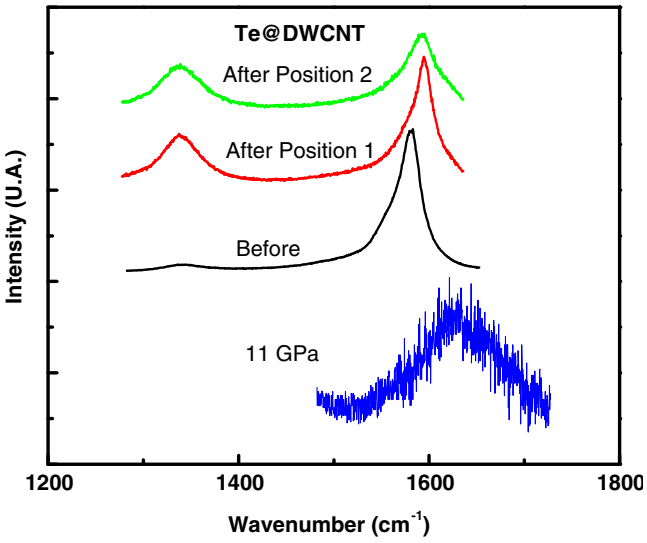

Fig. 8 – Raman spectra of the Te-filled DWCNTs before and after the pressure cycle in two different positions of the recovered sample. For comparison we see the Raman spectrum of the nanotubes at 11 GPa.

intensity when compared with the Raman spectrum of nanotubes before the pressure cycle (Fig. 8). Similar results were obtained in Ref. [27] reporting the synthesis of super-hard phases in CNTs.

4. Conclusion

In first instance the adopted chemical wetting method was successful and Tellurium entered almost all as trigonal Te inside DWCNTs giving the opportunity to distinguish pressure-induced spectral changes from internal and external walls in MWCNTs. The splitting of the G band can be explained by considering a tangential discontinuity of the stress component as one goes from the external wall to the internal one. At normal pressure, in addition to the radial modes of CNTs, we observed the Raman modes of Tellurium confined in CNTs. This confinement modifies the selection rules of the Tellurium phonons in the center of the Brillouin zone. Under pressure, we note that the pressure coefficient of the G bands of the internal and external CNTs filled with trigonal Te are larger than the pressure coefficients of empty CNTs and this has been attributed to the effect of charge transfer of electrons from the Tellurium nanowires to the CNTs. Finally, we unravel that the outer tubes act as a protection shield for the inner tubes (at least up to 11 GPa).

Acknowledgements

This research was supported in part by the Franco-Venezuelian Cooperation Program PCP "Nanotubos de Carbono". EB acknowledge support of this research to CDCHT-ULA (C-1683-09-05-B). M.M., J.G., F.R. and R.V. acknowledge support of this research by the MALTA-Consolider Ingenio 2010 Program.

REFERENCES

[1] Flahaut E, Bacsa R, Peigney A, Laurent C. Gram-scale CCVD synthesis of double walled carbon nanotubes. Chem Commun 2003(12):1442–3.
[2] Brown G, Bailey S, Novotny M, Carter R, Flahaut E, Coleman K, et al. High yield incorporation and washing properties of halides incorporated into single walled carbon nanotubes. Appl Phys A: Mater Sci Process 2003;76(4):457–62.
[3] Flahaut E, Sloan J, Friedrichs S, Kirkland A, Coleman K, Williams V, et al. Crystallization of 2H and 4H PbI_2 in carbon nanotubes of varying diameters and morphologies. Chem Mater 2006;18(8):2059–69.
[4] Monthioux M, Kuznetsov V. Who should be given the credit for the discovery of carbon nanotubes? Carbon 2006;44(9):1621–3.
[5] Kudryavstev A. The chemistry and technology of selenium and tellurium. London: Collet's Ltd.; 1974.
[6] Tsiulyanu D, Tsiulyanu A, Liess H, Eisele I. Characterization of tellurium-based films for NO_2 detection. Thin Solid Films 2005;485(1–2):252–6.
[7] Miura N, Tanaka S. Fast photoconductivity of tellurium by CO_2 laser radiation. Appl Phys Lett 1968;12(11):374–5.
[8] Zhuang F, Wu L, He S. Band structures of two-dimensional photonic crystals with regular polygon cylinders calculated by linear operations. Acta Phys Sin 2002;51(12):2865–70.
[9] Wilson H, Gutierrez W. Tellurium tft's exceed 100-MHz and one-watt capabilities. Proc IEEE 1967;55(3):415–6.
[10] Ju S, Janes DB, Lu G, Facchetti A, Marks TJ. Effects of bias stress on Zno nanowire field-effect transistors fabricated with organic gate nanodielectrics. Appl Phys Lett 2006;89(19):193506.
[11] Cao H, Qiu X, Liang Y, Zhu Q, Zhao M. Room-temperature ultraviolet-emitting In2O3 nanowires. Appl Phys Lett 2003;83(4):761–3.
[12] Li Z, Chen Y, Li X, Kamins T, Nauka K, Williams R. Sequence specific label-free DNA sensors based on silicon nanowires. Nano Lett 2004;4(2):245–7.
[13] Law JBK, Thong JTL. Simple fabrication of a Zno nanowire photodetector with a fast photoresponse time. Appl Phys Lett 2006;88(13):133114.
[14] Zhou W, Vavro J, Nemes NM, Fischer, Borondics F, Kamarás K, et al. Charge transfer and fermi level shift in *p*-doped single-walled carbon nanotubes. Phys Rev B 2005;71(20):205423.
[15] Chan CT, Kamitakahara WA, Ho KM, Eklund PC. Charge transfer effects in graphite intercalates: Ab initio calculations and neutron-diffraction experiment. Phys Rev Lett 1987;58(15):1528–31.
[16] Jorge J, Flahaut E, Gonzalez-Jimenez F, Gonzalez G, Gonzalez J, Belandria E, et al. Preparation and characterization of alpha-Fe nanowires located inside double wall carbon nanotubes. Chem Phys Lett 2008;457(4–6):347–51.
[17] Dresselhaus M, Eklund P. Phonons in carbon nanotubes. Adv Phys 2000;49(6):705–814.
[18] Dresselhaus MS, Dresselhaus G, Saito R, Jorio A. Raman spectroscopy of carbon nanotubes. Phys Rep 2005;409:47–99.
[19] Pine AS, Dresselhaus G. Raman spectra and lattice dynamics of tellurium. Phys Rev B 1971;4(2):356–71.
[20] Puech P, Bassil A, Gonzalez J, Power C, Flahaut E, Barrau S, et al. Similarities in the Raman RBM and D bands in double-wall carbon nanotubes. Phys Rev B 2005;72(15):155436.
[21] Puech P, Hubel H, Dunstan DJ, Bacsa RR, Laurent C, Bacsa WS. Discontinuous tangential stress in double wall carbon nanotubes. Phys Rev Lett 2004;93(9):095506.
[22] Arvanitidis J, Christofilos D, Papagelis K, Andrikopoulos KS, Takenobu T, Iwasa Y, et al. Pressure screening in the interior of primary shells in double-wall carbon nanotubes. Phys Rev B 2005;71(12):125404.
[23] Hanfland M, Beister H, Syassen K. Graphite under pressure: equation of state and first-order Raman modes. Phys Rev B 1989;39(17):12598–603.
[24] Peters MJ, McNeil LE, Lu JP, Kahn D. Structural phase transition in carbon nanotube bundles under pressure. Phys Rev B 2000;61(9):5939–44.
[25] Gonzalez J, Power C, Belandria E, Jorge J, Gonzalez-Jimenez F, Millot M, et al. Pressure dependence of Raman modes in double wall carbon nanotubes filled with alpha-Fe. High Pressure Res 2008;28(4):577–82.
[26] Puech P, Ghandour A, Sapelkin A, Tinguely C, Flahaut E, Dunstan DJ, et al. Raman G band in double-wall carbon nanotubes combining p doping and high pressure. Phys Rev B 2008;78(4):045413.
[27] Popov M, Kyotani M, Nemanich RJ, Koga Y. Superhard phase composed of single-wall carbon nanotubes. Phys Rev B 2002;65(3):033408.